Analysis of Magnetic Plates Attached to a Deflection Yoke with a Hybrid Method

TAKAFUMI NAKAGAWA, SOICHIRO OKUDA, HIROAKI NISHINO, MICHIO OGASA, AND TAKEO FUJIMURA

Abstract—**Deflection yokes require several kinds of magnetic plates to correct the misconvergence of three beams. The effects of magnetic plates attached to a deflection yoke were simulated with a computer program. In this program the magnetic fields were computed with a hybrid method combining a surface-charge method with a finite-difference method using Fourier transformation. The misconvergence pattern changed by a silicon steel plate attached to a deflection yoke was calculated by this program. Although the calculated vertical misconvergence changes were larger than the measurements, the horizontal misconvergence changes agreed with the measured misconvergence changes within the experimental errors. This result shows that the developed computer program would be efficient for designing the deflection yokes with optimum magnetic plates.**

I. Introduction

DEFLECTION yokes (DY's) used for cathode ray tubes (CRT's) require several kinds of magnetic plates:

1) In assembling a DY with a CRT, the deviations of the manufacturing process can cause a discrepancy between the axes of the DY and the CRT. This discrepancy makes it necessary to use correction magnetic plates.
2) A self-convergence DY for a CRT with a wide deflection angle often requires magnetic plates since the coils of a DY cannot generate a special local magnetic field.

Although the design and assembly are currently based on the experience of the designers and workers, the demand for better DY's and CRT's requires optimizing the design of these magnetic plates based on analysis. By using computer modeling, we can obtain the optimum shape of a magnetic plate and its optimum location in designing and assembling a DY. We can make the data base for the process of assembling a DY to a CRT without experiments and can automate the assembling process. Moreover, we can intentionally install magnetic plates from the stage of designing a DY with computer modeling. Some of these magnetic plates control the vertical magnetic field to keep self-convergence over the screen without deteriorating raster distortion.

In order to analyze the magnetic fields of a DY, a finite-difference method with a Fourier transformation was developed [1]. Although this method developed as a good tool for designing the windings of the main coils of a DY, it cannot take into account magnetic plates that are not rotationally symmetric.

We have developed a computer program that calculates the magnetic fields by a hybrid method that combines a finite-difference method (FDM) with a surface-charge method (SCM), a kind of a boundary-elements method. Although SCM is restricted in linear problems, its calculations are fast and exact, and it can handle a general three-dimensional (3D) configuration. This program also calculates the misconvergence, i.e., the discrepancies of the spot locations on the screen, by tracing the three beams.

The solution of this program was compared with the misconvergence pattern by measuring a model CRT.

II. Hybrid Method

In this section, the algorithm of the developed program will be described.

A. Field Calculation

The total magnetic field $\boldsymbol{H}$ is the sum of the magnetic field $\boldsymbol{H}_c$ generated by the main coil of the DY and the magnetic field $\boldsymbol{H}_m$ by the magnetization of magnetic plates.

$$\boldsymbol{H} = \boldsymbol{H}_c + \boldsymbol{H}_m. \tag{1}$$

The main field $\boldsymbol{H}_c$ was calculated following the algorithm developed for current distributions on revolving surfaces [1]. By this method the distribution of the coils is replaced by current sheets, and the Poisson equation is discretized by a finite-difference method. These approximations allow the use of the scalar potential ϕ in the whole space.

In order to reduce the three-dimensional problem to a two-dimensional (rotationally symmetric) problem, the scalar potentials and the current distributions are ex-

Manuscript received October 25, 1988; revised June 6, 1989.

T. Nakagawa and S. Okuda are with the Central Research Laboratory, Mitsubishi Electric Corporation, 1-1 Tsukaguchihonmachi 8 Chome, Amagasaki 661, Japan.

H. Nishino, M. Ogasa, and T. Fujimura are with the Kyoto Works, Mitsubishi Electric Corporation, 1 Babuzusho Nagaokakyo 617, Japan.

IEEE Log Number 8929840.

panded in Fourier series with regard to the azimuthal angle θ as follows:

$$i(r, \theta, z) = i_1(r, z) \cos \theta + i_3(r, z) \cos 3\theta + i_5(r, z) \cos 5\theta + \cdots \quad (2)$$

$$\phi(r, \theta, z) = \phi_1(r, z) \sin \theta + \phi_3(r, z) \sin 3\theta + \phi_5(r, z) \sin 5\theta + \cdots . \quad (3)$$

The final equation is a system of simultaneous linear equations. An iterartive algorithm is used to solve a simultaneous linear equation. The magnetic field of an arbitrary location is calculated by differentiating the scalar potential ϕ.

B. Magnetic Field Generated by Magnetic Plates

The magnetic field generated by magnetic plates was calculated by a surface-charge method [2]. In this method, virtual magnetic charges on the surface of a ferromagnetic material are assumed. The magnetic field $\boldsymbol{H}_m$ by the ferromagnetic material is calculated by summing the contributions of the virtual charges.

$$\boldsymbol{H}_m = -\frac{1}{4\pi\mu_0} \int_s \operatorname{grad} \frac{\sigma}{r}\, dS \quad (4)$$

where r is a distance from a point on the surface of the ferromagnetic material to a calculated point.

An integral equation is derived from the continuity of the normal component of the magnetic field on the boundary surface between the ferromagnetic material and air.

$$\boldsymbol{H} \cdot \boldsymbol{n}\big|_{\text{out}} = \boldsymbol{H} \cdot \boldsymbol{n}\big|_{\text{in}} \quad (5)$$

where subscripts "out" and "in" denote the magnetic field of the outside and inside regions of the ferromagnetic material, respectively.

Using (1), we reform (5) as follows:

$$\boldsymbol{H} \cdot \boldsymbol{n}\big|_{\text{out}} = \boldsymbol{H}_c \cdot \boldsymbol{n}\big|_{\text{in}} + \boldsymbol{H}_m \cdot \boldsymbol{n}\big|_{\text{in}}. \quad (6)$$

The second term in the right-hand side of the equation $\boldsymbol{H}_m \cdot \boldsymbol{n}\big|_{\text{in}}$ is calculated by dividing the boundary surface into small surface elements where the magnetic charge density σ is assumed to be constant.

$$\boldsymbol{H}_m \cdot \boldsymbol{n}\big|_{\text{in}} = -\frac{\sigma_{(i)}}{2\mu_0} - \sum_{j \neq i} \frac{\sigma^{(j)}}{4\pi\mu_0} \int_{s^{(j)}} \operatorname{grad} \frac{1}{r}\, dS \cdot \boldsymbol{n}. \quad (7)$$

The first and second terms of the right-hand side of (7) are the magnetic field produced by magnetic charge on a small surface element under consideration and on the outside elements, respectively.

Since $\boldsymbol{H} \cdot \boldsymbol{n}\big|_{\text{out}}$ is calculated from the susceptibility χ_s

$$\boldsymbol{H} \cdot \boldsymbol{n}\big|_{\text{out}} = \frac{\sigma_{(i)}}{\chi_s \mu_0} \quad (8)$$

the following equation results from (5)–(8):

$$\frac{\sigma_{(i)}}{\chi_s \mu_0} = \boldsymbol{H}_c \cdot \boldsymbol{n} + \left(-\frac{\sigma_{(i)}}{2\mu_0}\right) - \sum_{j \neq i} \frac{\sigma^{(j)}}{4\pi\mu_0} \int_{s^{(j)}} \operatorname{grad} \frac{1}{r}\, dS \cdot \boldsymbol{n}. \quad (9)$$

From this equation we obtain the following system of simultaneous equation:

$$A \cdot \vec{\sigma} = \vec{b} \quad (10)$$

where $\vec{\sigma}$ is a vector of unknown charge densities, $\vec{b}$ is a vector of known external field having the elements b_i:

$$b_i = -\boldsymbol{H}_c^{(i)} \cdot \boldsymbol{n}^{(i)} \quad (11)$$

and $\boldsymbol{A}$ is a matrix having the elements a_{ij} defined as follows:

$$a_{ii} = -\frac{1}{\mu_0}\left(\frac{1}{2} + \frac{1}{\chi_s}\right) \quad (12)$$

$$a_{ij} = -\frac{1}{4\pi\mu_0} \int_{s^{(j)}} \operatorname{grad} \frac{1}{r}\, dS \cdot \boldsymbol{n}. \quad (13)$$

C. Program

In this section, the algorithm of the developed program is described. The flow chart of this program is shown in Fig. 1.

This program is composed of three parts. The first part is the calculation of the main magnetic field $\boldsymbol{H}_c$ by a finite-difference method with a Fourier expansion. The second part is the calculation of the surface magnetic charge distribution on the surface and magnetic field $\boldsymbol{H}_m$ generated by the magnetization of ferromagnetic materials by SCM. The last part is the trace of three beam trajectories.

The calculation area is divided into small meshes based on input data (I), the deflection yoke scheme, and, boundary condition. The current distribution is expanded in Fourier series in advance. The magnetic scalar potential is calculated for each harmonic. The main magnetic field $\boldsymbol{H}_c$ is computed by these potential data results.

In the next step, data (III), the magnetic plate scheme, the gun, and the screen position are input to compute a misconvergence on the screen of the CRT. As we can calculate the field $\boldsymbol{H}_c$ at each mesh on the surface, the surface magnetic charge distributions on the surface of magnetic plates can be obtained by solving (10).

Since the deflection magnetic field generated by a DY is computed with (1) with the magnetic scalar potentials and charges, we can obtain the misconvergence patterns by tracing beam trajectories with a Runge–Kutta method. There is an output of the deflection magnetic field as an option.

III. Experiment

This program was verified by comparing its results with the measurements. The object of the verification is the

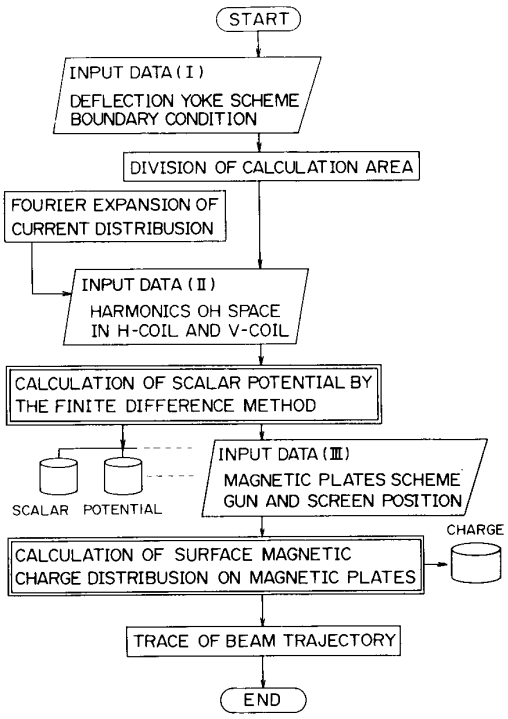

Fig. 1. Flow chart of the developed program. This program is composed of three parts. The magnetic fields generated by coils and a magnetization of ferromagnetic material are calculated, and misconvergence on the screen is obtained by tracing the three beams.

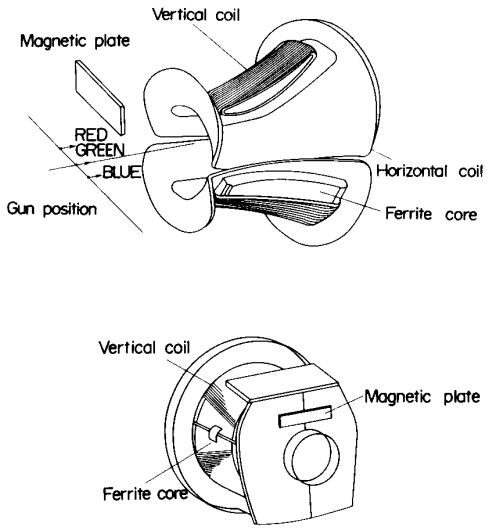

Fig. 2. Schematic drawing of the model deflection yoke with a correction magnetic plate at the entrance. The DY has a pair of saddle-shaped line (horizontal) coils, a pair of troid-shaped field (vertical) coils, and a conical ferrite core. The block-shaped magnetic plate is made of silicon steel and used for correction of the discrepancy between the axes of the DY and the CRT.

effect of a magnetic plate attached to a DY as shown in Fig. 2.

The change of the misconvergence pattern on a CRT screen caused by this magnetic plate installed at the entrance of an actual DY was measured and compared with the calculated pattern by tracing the three beams.

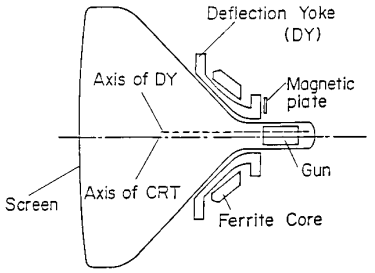

Fig. 3. The discrepancy between axes of the CRT and of the DY. Since the axis of DY is above the axis of CRT, the magnetic plate is attached at the upper side of the DY.

A. Effects of Magnetic Plate

Magnetic plates are commonly used for correcting the discrepancy between the axes of a CRT and of a DY in the assembly process shown in Fig. 3. The principle of its effect is shown in Fig. 4.

When the axis of a DY shifts vertically from the axis of a CRT, the misconvergence pattern shown in the left drawing of Fig. 4(a) is observed. The outer beam separates horizontally in the counter direction between the top and the bottom areas of the screen.

The reason of this separation is shown in the drawing on the right-hand side of Fig. 4(a). When the beams are deflected upward, the outer beams are forced inward when they pass the strongest main field. This force makes the order of the spots at the screen contrary to the electron beams. When the beams are deflected downward, the beams are forced to outward, and the order of the spots on the screen is the same as with the order of the electron beams.

This pattern is often observed in installing a DY to a CRT and is corrected by attaching a magnetic plate to the DY above the axis as shown in Fig. 2.

The reason for this correction is shown in the right-hand drawing of Fig. 4(b). Since the magnetic plate gathers the leakage magnetic fluxes and increases the curvature of the flux lines, the center of the magnetic flux moves downward. This makes the center of the flux lines coincide with the axis of the CRT and corrects the misconvergence pattern.

B. Measurement of Misconvergence Pattern

We measured the misconvergence values of a test CRT with a test DY for both with and without the magnetic plate. The size of the magnetic plate is 29 mm long, 5 mm wide, and 0.5 mm thick.

The specification of the test CRT is as follows:

Screen Size	1 V
Scanning Frequency of Horizontal Deflection	24 kHz
Mask Pitch	0.31 mm

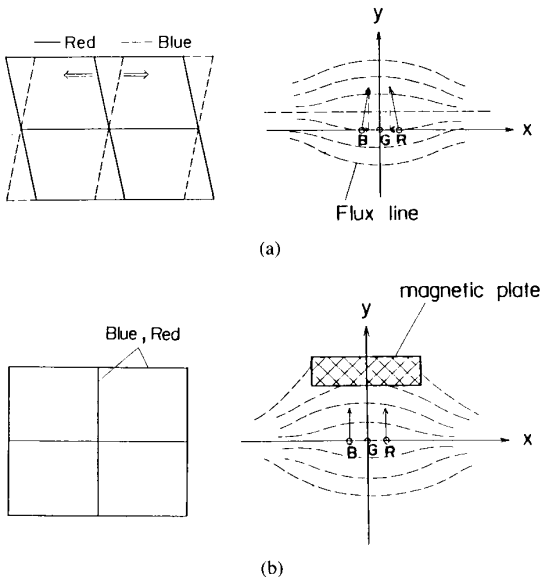

Fig. 4. Schematic drawings of effect of magnetic plate. (a) Misconvergence pattern and magnetic flux line. The center of vertical deflecting field locates vertically away from the axis of the CRT. (b) Misconvergence pattern and magnetic flux line when a magnetic plate is attached to a DY as shown in Fig. 2. The center of the field coincides with the axis of the CRT.

Type of Phosphor	Dots
Usage	Data display

The devices usually installed in the electron gun for magnetically correcting coma aberration was intentionally removed for conforming to the assumption of the calculation.

The specification of the test DY is as follows:

Deflection Angle	90 degrees
Horizontal Winding	Saddle
Vertical Winding	Torroid

A pair of magnetic devices (rear arms) and a correction device (dynamic differential convergence unit) usually installed in this DY were intentionally removed to conform to the assumption of the calculation.

The misconvergence values were measured by using a 25× power microscope. The resolving power of this measurement was 0.05 mm.

IV. Results and Discussions

A. Measurement

The misconvergence value was defined as the location of the spot of an outer beam (red or blue) relative to the spot of the center beam (green). In order to evaluate the effect of the magnetic plate, the change of the misconvergence values were calculated by subtracting the misconvergence values without the magnetic plate from the misconvergence values with the magnetic plate.

$$\Delta X_{B-G} = (X_{BW} - X_{GW}) - (X_{BO} - X_{GO}) \quad (14)$$

$$\Delta Y_{B-G} = (Y_{BW} - Y_{GW}) - (Y_{BO} - Y_{GO}) \quad (15)$$

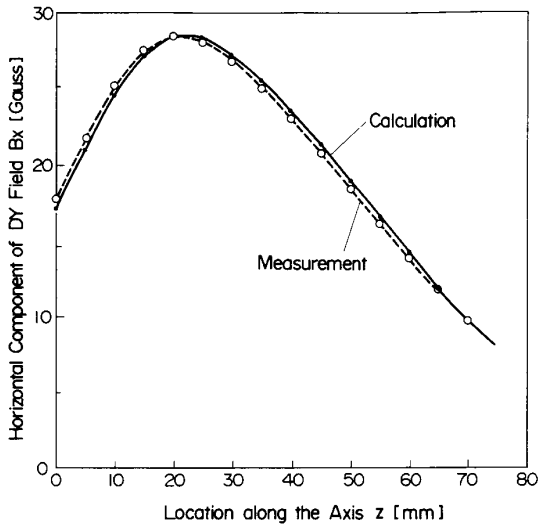

Fig. 5. The distribution of the horizontal component of magnetic fields along the axis of the DY. Solid and dashed lines show the calculated values and measured values, respectively.

$$\Delta X_{R-G} = (X_{RW} - X_{GW}) - (X_{RO} - X_{GO}) \quad (16)$$

$$\Delta Y_{R-G} = (Y_{RW} - Y_{RW}) - (Y_{RO} - Y_{GO}) \quad (17)$$

where X and Y are horizontal and vertical coordinates on the screen, respectively. The subscripts R, G, and B denote red, green, and blue beams, and the subscripts W and O denote with and without a magnetic plate, respectively.

B. Calculation

The misconvergence patterns with and without the magnetic plate were calculated by tracing the electron beams based on the field computation described in Section II. The distribution of the calculated flux densities of the vertical deflection coil is shown in Fig. 5 compared with the measured values. The calculation, finite difference with Fourier transformation, gives good agreement with the measurement.

The leakage flux at $z = -8$, the location of the correction magnetic plate, is less than 18 G. Since this level of mgnetic flux is far below the saturation region, it is a good assumption that the field computation is in the linear portion of the B-H curve and the SCM is feasible. The horizontal deflection field was treated in the same way.

The surface of the magnetic plate was divided into rectangular elements for SCM. Since the magnetic plate was thin and the charges induced on the surface elements would be nearly equal and opposite in sign on two sides, the opposite surfaces were divided so as to locate the elements of every other surface alternately as shown in Fig. 6. This division enabled us to avoid numerical round-off errors.

C. Comparison

The calculated changes of the misconvergence ΔX and ΔY in (14)–(17) were compared with the measured values and are illustrated in Fig. 7.

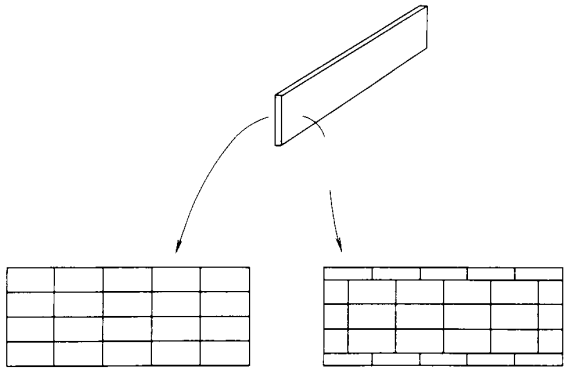

Fig. 6. Schematic drawing of the divided elements on the surface of the magnetic plate. The front and rear surfaces of the magnetic plate are differently divided so as to alternatively locate each element of opposite side.

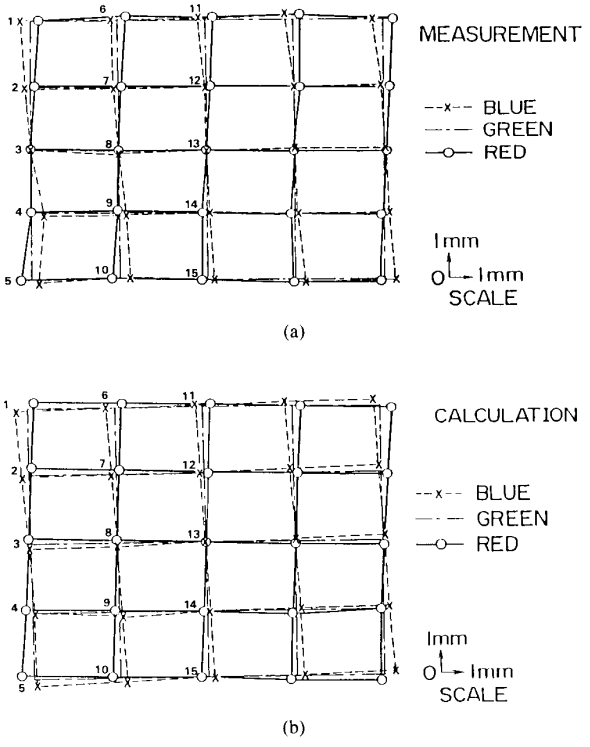

Fig. 7. The change of the misconvergence pattern caused by the magnetic plate. (a) The measured shifts of the outer beam spots relative to the central (green) beam measured on the whole screen. (b) The calculated shifts.

Table I gives a summary of the comparison. The results show that the calculated values and the measurements agree quite well especially along the central vertical line of the screen, i.e., when the horizontal deflecting coils are not excited. The difference is within the experimental errors.

These results show that the main purpose described in Section III-A was well simulated by the computer program. This program proved to be applicable to the optimum configuration of the magnetic plates for correcting misconvergence. The agreement of the vertical change of misconvergence ("ΔY" in Table I) is rather poor along the outer vertical lines of the screen. The calculated change of misconvergence is larger than the measured values by more than the experimental errors. The possible reasons of this discrepancy could be as follows:

1) The attachment of the magnetic plate to a DY may cause a change in the inductance of the coil nearby.
2) A frequency of the horizontal deflection field higher than the vertical deflection field may result in a significant difference from the static field assumed in the calculation.
3) The leakage flux of the horizontal deflection field is weaker than the leakage flux of the vertical deflection field. This weakness may cause the loss of significant digits in computation.

The changes of inductances of horizontal deflection coils due to the magnetic plate were measured to examine possible reason 1). The results showed that attaching the magnetic plate at the top of the DY increases the inductance of top deflection coil while it decreases the inductance of the bottom coil. This difference between the inductances of these coils causes the difference between the currents of the two coils and increases the function of the magnetic plate. This effect contradicts the result that the calculated values are larger than the measured values. Therefore, the change of inductance cannot be the reason for the discrepancy between calculation and measurement.

The frequency effect (see 2)) was examined by measuring the misconvergence values with the static deflection field. The results showed that the effects of the magnetic plate are not significantly different from the effects measured with the dynamic deflection field.

The leakage flux densities from the excited coils were measured to examine reason 3). The results showed that the leakage flux density from the horizontal deflection coil is 2 G, whereas the leakage flux density from the vertical deflection coil is 16 G. This difference between the leakage flux densities from the horizontal and vertical coils would be the only reason remaining to explain the poor agreement of the vertical change of the misconvergence. The reasons are not yet clear and are subject to future studies.

V. Conclusions

A hybrid method combining the surface-charge method with a finite-different method was developed for analyzing the effect of magnetic plates attached to a deflection yoke. This method was used to analyze the effect of a correction magnetic plate attached outside of a DY. By comparing the change of the misconvergence pattern with the measurement, the following conclusions were drawn:

TABLE I
CHANGE OF THE MISCONVERGENCE VALUES

Location	BLUE-GREEN X		BLUE-GREEN Y		RED-GREEN X		RED-GREEN Y	
	Calc.	Meas.	Calc.	Meas.	Calc.	Meas.	Calc.	Meas.
11	-0.33	-0.34	0.14	0.12	0.33	0.35	0.14	0.12
12	-0.17	-0.07	0.05	0.00	0.17	0.20	0.05	0.00
13	0.00	0.00	0.00	0.00	0.00	0.00	0.00	0.00
14	0.16	0.12	-0.05	0.00	-0.16	-0.18	-0.05	0.00
15	0.30	0.33	-0.06	-0.05	-0.30	-0.22	-0.06	-0.05
1	-0.53	-0.48	-0.10	0.07	0.32	0.37	0.29	0.07
2	-0.27	-0.23	-0.11	-0.07	0.12	0.20	0.29	0.08
3	-0.07	-0.03	-0.20	-0.05	-0.10	-0.05	0.23	0.12
4	0.13	0.55	-0.00	-0.13	-0.27	0.00	0.15	0.09
5	0.17	0.33	-0.30	-0.17	-0.50	-0.47	0.15	-0.02

The numbers of locations correspond to the numbers in Fig.7. Numbers from 11 to 15 correspond to the spots along the central vertical line, and from 1 to 5 correspond to the spots along the outer line of the screen.

1) The calculated change of the horizontal misconvergence values agreed with the measurement within the experimental errors.
2) The calculated change of the vertical misconvergence values agreed with the measurement when the horizontal deflection field is not invoked.
3) The calculation given significantly larger amount of vertical misconvergence change than the measurement when the horizontal deflection field is invoked.
4) The computer program developed with this hybrid method proved to be efficient for designing high-performance deflection yokes with magnetic plates.

REFERENCES

[1] T. Nomura, *Trans. IEE Japan*, vol. 91, pp. 155-163, 1971.
[2] S. Nakamura, T. Nomura, and M. Iwamoto, *Trans. IEE Japan*, vol. 96, pp. 55-62, 1976.

*

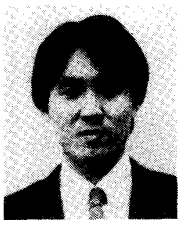

Takafumi Nakagawa was born in Kumamoto Prefecture, Japan, on August 31, 1958. He received the B.E. degree in the mechanical engineering from Doshisha University and the M.E. degree in applied physics from Miyazaki University, Japan, in 1982 and in 1984, respectively.

Since 1984, he has been working in the Central Research Laboratory, Mitsubishi Electric Corporation, where he has been engaged in the research of magnetic field analysis and the development of computer programs.

Mr. Nakagawa is a member of the Institution of Electrical Engineers of Japan and of the Physics Society of Japan.

*

Soichiro Okuda was born in Ooita Prefecture, Japan, on April 11, 1949. He received the B.E. and M.E. degrees in applied mathematics from the University of Tokyo, Tokyo, Japan, in 1973 and 1975, respectively.

Since 1975, he has been working in the Central Research Laboratory, Mitsubishi Electric Corporation. After conducting research on switch gears and plasma for five years, he has been working on the beam dynamics based on field analysis.

Mr. Okuda is a member of the Institute of Electrical Engineers of Japan and the Institute of Electronics and Communication Engineers of Japan.

*

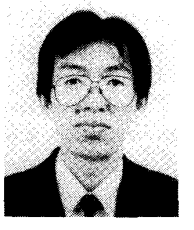

Hiroaki Nishino was born in Toyama Prefecture, Japan, on May 25, 1962. He received the B.E. degree in electrical engineering from Kanazawa University, Japan, in 1985.

Since 1985, he has been working in the Kyoto Works, Mitsubishi Electric Corporation, where he has been engaged in the design of deflection yokes.

Mr. Nishino is a member of the Institute of Electrical Engineers of Japan.

*

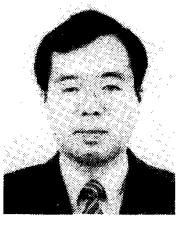

Michio Ogasa was born in Aichi Prefecture, Japan, on June 22, 1953. He received the B.E. and M.E. degrees in electrical engineering from Nagoya University, Japan, in 1976 and 1978, respectively.

Since 1978, he has been working in the Kyoto Works, Mitsubishi Electric Corporation, where he has been engaged in the design of deflection yokes.

*

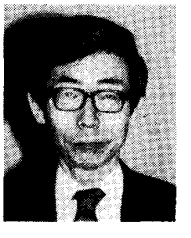

Takeo Fujimura was born in Mie Prefecture, Japan, on December 23, 1937. He received the B.E. degree from Shizuoka University, Japan, in 1960.

He has been working in the Kyoto Works, Mitsubishi Electric Corporation, where he has been engaged in the design of shadow-mask tubes.

Mr. Fujimura is a member of the Institute of Television Engineers of Japan.